

Supporting Information

Development of an Aptamer-based Sensing Platform for Metal Ions, Proteins and Small Molecules Through Terminal Deoxynucleotidyl Transferase-induced G-quadruplex Formation

Ka-Ho Leung,[†] Bingyong He,[†] Chao Yang,[§] Chung-Hang Leung,^{*,§} Hui-Min David Wang,^{*,||} and Dik-Lung Ma^{*,†,‡}

[†]Department of Chemistry, Hong Kong Baptist University, Kowloon Tong, Hong Kong
E-mail: edmondma@hkbu.edu.hk

[§]State Key Laboratory of Quality Research in Chinese Medicine, Institute of Chinese Medical Sciences, University of Macau, Macao E-mail: duncanleung@umac.mo

^{||}Graduate Institute of Natural Products, Kaohsiung Medical, University, Kaohsiung 807, Taiwan E-mail: davidw@kmu.edu.tw

[‡]Partner State Key Laboratory of Environmental and Biological Analysis, Hong Kong Baptist University, Hong Kong, China

Experimental section

Materials. Reagents, unless specified, were purchased from Sigma Aldrich (St. Louis, MO) and used as received. Iridium chloride hydrate ($\text{IrCl}_3 \cdot x\text{H}_2\text{O}$) was purchased from Precious Metals Online (Australia). Exonuclease I (ExoI), terminal deoxynucleotidyl transferase (TdT), dGTP and dATP was purchased from New England Biolabs Inc. (Beverly, MA, USA). All oligonucleotides were synthesized by Techdragon Inc. (Hong Kong, China).

General experimental

Mass spectrometry was performed at the Mass Spectroscopy Unit at the Department of Chemistry, Hong Kong Baptist University, Hong Kong (China). Deuterated solvents for NMR purposes were obtained from Armar and used as received.

^1H and ^{13}C NMR were recorded on a Bruker Avance 400 spectrometer operating at 400 MHz (^1H) and 100 MHz (^{13}C). ^1H and ^{13}C chemical shifts were referenced internally to solvent shift (acetone- d_6 : ^1H δ 2.05, ^{13}C δ 29.8; CD_3Cl : ^1H δ 7.26, ^{13}C δ 76.8). Chemical shifts (δ) are quoted in ppm, the downfield direction being defined as positive. Uncertainties in chemical shifts are typically ± 0.01 ppm for ^1H and ± 0.05 for ^{13}C . Coupling constants are typically ± 0.1 Hz for ^1H - ^1H and ± 0.5 Hz for ^1H - ^{13}C couplings. The following abbreviations are used for convenience in reporting the multiplicity of NMR resonances: s, singlet; d, doublet; t, triplet; q, quartet; m, multiplet; br, broad. All NMR data was acquired and processed using standard Bruker software (Topspin).

Photophysical measurement

Emission spectra and lifetime measurements for complexes were performed on a PTI TimeMaster C720 Spectrometer (Nitrogen laser: pulse output 337 nm) fitted with a 380 nm filter. Error limits were estimated: λ (± 1 nm); τ ($\pm 10\%$); ϕ ($\pm 10\%$). All

solvents used for the lifetime measurements were degassed using three cycles of freeze-vac-thaw.

Luminescence quantum yields were determined using the method of Demas and Crosby¹ [Ru(bpy)₃][PF₆]₂ in degassed acetonitrile as a standard reference solution ($\Phi_r = 0.062$) and calculated according to the following equation:

$$\Phi_s = \Phi_r(B_r/B_s)(n_s/n_r)^2(D_s/D_r)$$

where the subscripts s and r refer to sample and reference standard solution respectively, n is the refractive index of the solvents, D is the integrated intensity, and Φ is the luminescence quantum yield. The quantity B was calculated by $B = 1 - 10^{-AL}$, where A is the absorbance at the excitation wavelength and L is the optical path length.

Synthesis

The following complexes were prepared according to (modified) literature methods. All complexes are characterized by ¹H NMR, ¹³C NMR, high resolution mass spectrometry (HRMS) and elemental analysis.²

Complex 1. ¹H NMR (400 MHz, Acetone-*d*₆) δ 8.97 (d, $J = 8.8$ Hz, 2H), 8.91 (d, $J = 8.8$ Hz, 2H), 8.15-8.05 (m, 8H), 7.90-7.86 (m, 2H), 7.71 (d, $J = 8.0$ Hz, 2H), 7.66-7.62 (m, 2H), 7.27-7.23 (m, 2H), 7.05-7.01 (m, 2H), 6.87 (dd, $J_1 = 1.6$ Hz $J_2 = 8.0$ Hz, 2H), 6.17 (d, $J = 1.2$ Hz, 2H), 2.43-2.29 (m, 4H), 1.02 (t, $J = 7.6$ Hz, 6H); ¹³C NMR (100 MHz, Acetone-*d*₆) 168.5, 161.1, 151.3, 149.7, 149.0, 147.6, 142.1, 142.0, 139.3, 131.9, 131.4, 130.9, 129.9, 129.7, 129.2, 125.9, 123.6, 123.2, 122.9, 120.29, 29.8, 18.6; MALDI-TOF-HRMS: Calcd. for C₄₄H₃₆IrN₄[M-PF₆]⁺ : 813.2569 Found: 813.3104; Anal.: (C₄₄H₃₆IrN₄PF₆ +H₂O) C, H, N: calcd. 54.15, 3.92, 5.74; found. 54.29, 3.8, 5.92.

Complex 2. Reported.³

Complex 3. Reported.³

Luminescence response of Ir(III) complexes 1–3 towards different forms of DNA

The G-quadruplex DNA-forming sequence (Pu27) was annealed in Tris-HCl buffer (20 mM Tris, 100 mM KCl, pH 7.0) and were stored at $-20\text{ }^{\circ}\text{C}$ before use. Complex 1–3 (1 μM) was added to 5 μM of ssDNA, dsDNA or Pu27 G-quadruplex DNA in Tris-HCl buffer (20 mM Tris, pH 7.0).

Detection of thrombin, cocaine and K^+

To a 30 μL solution of Tris buffered solution (K^+ detection: 50 mM Tris-HCl, 2 mM MgCl_2 , pH 8.3; thrombin detection: 100 mM Tris, 140 mM NaCl, 20 mM MgCl_2 , 20 mM KCl; cocaine detection: 25 mM Tris-HCl, 0.15 M NaCl, 2 mM MgCl_2 , pH 8.0) with the indicated concentration of target was added the appropriate aptamer (1 μM). Then, ExoI (K^+ detection: 0.33 U/ μL ; thrombin detection: 0.33 U/ μL ; cocaine detection: 0.66 U/ μL) was added and the samples were incubated at $37\text{ }^{\circ}\text{C}$ for 30 min to allow DNA cleavage take place and the reaction was inactivated by heating at $80\text{ }^{\circ}\text{C}$ for 20 min. 5 μL 10 \times NEB TdT buffer, 250 μM CoCl_2 2.4 mM dGTP, 1.6 mM dATP and 0.33 U/ μL of TdT was added and the solution was made up with H_2O to 50 μL . After 1 h in $37\text{ }^{\circ}\text{C}$, the reaction was stopped by the addition of 25 μL 100 mM EDTA- Na_2 . The samples were added to 425 μL Tris-HCl buffer (20 mM Tris, 50 mM KCl, pH 7.2) and the resulting solutions were incubated for 30 min. Emission spectra were recorded in the 540–760 nm range using an excitation wavelength of 360 nm.

Table S1. DNA sequences used in this project:

	Sequence
cocaine aptamer	5'-GGGAGTCAAGAACAAAGTTCTTCAATGAAGTGTGGGACGA CA-3'
thrombin aptamer	5'-AGTCCGTGGTAGGGCAGGTTGGGGTGACT-3'
Pu27	5'-TGGGGAGGGTGGGGAGGGTGGGGAAGG-3'
Pu22	5'-TGAGGGTGGGGAGGGTGGGGAA-3'
ds17	5'-C ₂ AGT ₂ CGTAGTA ₂ C ₃ -3' 5'-G ₃ T ₂ ACTACGA ₂ CTG ₂ -3'
ssDNA	5'-C ₂ AGT ₂ CGTAGTA ₂ C ₃ -3'
ds26	5'-CAATCGGATCGAATTCGATCCGATTG-3'
F21T	5'-FAM-(G ₃ [T ₂ AG ₃] ₃)-TAMRA-3'
F10T	5'-FAM-TATAGCTA-HEG-TATAGCTATAT-TAMRA-3'

Table S2 Comparison of recently reported oligonucleotide-based universal detection platforms

Method	Modified DNA?	Exogenous reagent	Biological sample	Ref.
This study	No	ExoI, TdT, Selective G4 Ir(III) complex	Oral fluid, Cell extract,	
Self-assembled, functionalized graphene and DNA as a universal platform for colorimetric assays	No	Graphene oxide, H ₂ O ₂ , 3,3',5,5'-tetramethylbenzidine	-	4
Versatile DNAzyme-Based Amplified Biosensing Platforms for Nucleic Acid, Protein, and Enzyme Activity Detection	Yes	DNAzyme	Cellular homogenate	5
An ultrasensitive universal detector based on neutralizer displacement	Yes	DNA neutralizer	Unpurified lysates	6
Amplified Fluorescence Aptamer-Based Sensors Using Exonuclease III for the Regeneration of the Analyte	Yes	Exonuclease III	-	7
General Colorimetric Detection of Proteins and Small Molecules Based on Cyclic Enzymatic Signal Amplification and Hairpin Aptamer	Yes	Nanoparticles, nicking endonuclease	HeLa lysate -	8

Probe				
Label-Free Fluorescent Detection of Ions, Proteins, and Small Molecules Using structure-Switching Aptamers, SYBR Gold, and Exonuclease I	No	Exonuclease I, Non-selective SYBR Gold	Serum, urine	9
Colorimetric detection of DNA, small molecules, proteins, and ions using unmodified gold nanoparticles and conjugated polyelectrolytes	No	Nanoparticles, conjugated polymer	Serum	10

Table S3 Photophysical properties of novel iridium(III) complex **1**.

Complex	Quantum yield	λ_{em}/nm	Lifetime/ μs	UV/vis absorption λ_{abs}/nm ($\epsilon/\text{dm}^3\text{mol}^{-1}\text{cm}^{-1}$)
1	0.25937	651	5.2	215 (9.93×10^4), 270 (1.20×10^5), 365 (4.24×10^4), 370 (3.88×10^4)

Figure S1 (a) Chemical structure of complex **1**. (b) Luminescence response of complex **1** towards various DNA, (c) G4-FID titration curves of DNA duplex ds26, ds17 or G-quadruplex Pu27. (d) Melting profile of F21T G-quadruplex DNA (0.2 μM) in the absence and presence of **1** (3 μM). (e) Melting profile of F10T (0.2 μM) in the absence and presence of **1** (3 μM). (f) Melting profile of F21T G-quadruplex DNA (0.2 μM) in the absence and presence of **1** (5 μM) and ds26 (10 μM) or ssDNA (10 μM).

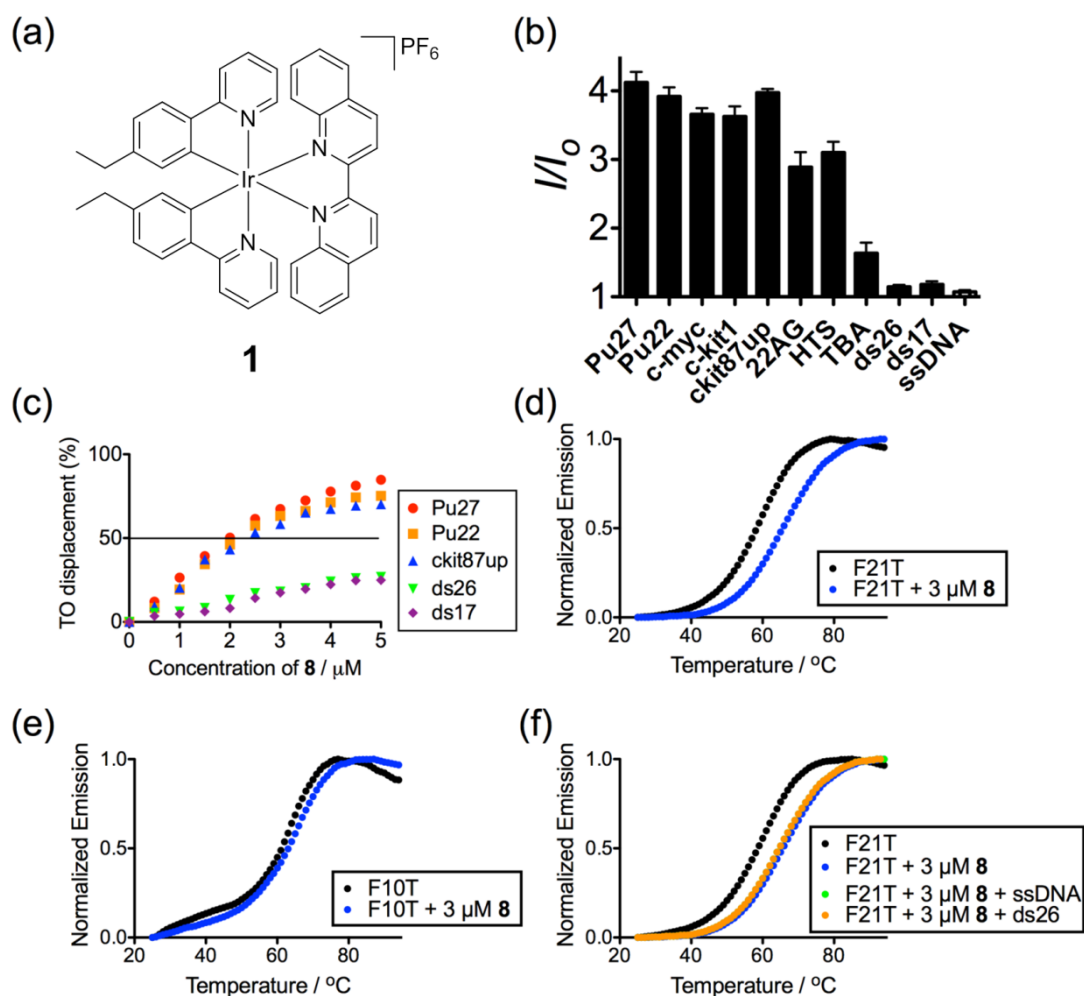


Figure S2 Luminescence enhancement of complex **1** as a function of loop size of central loop.

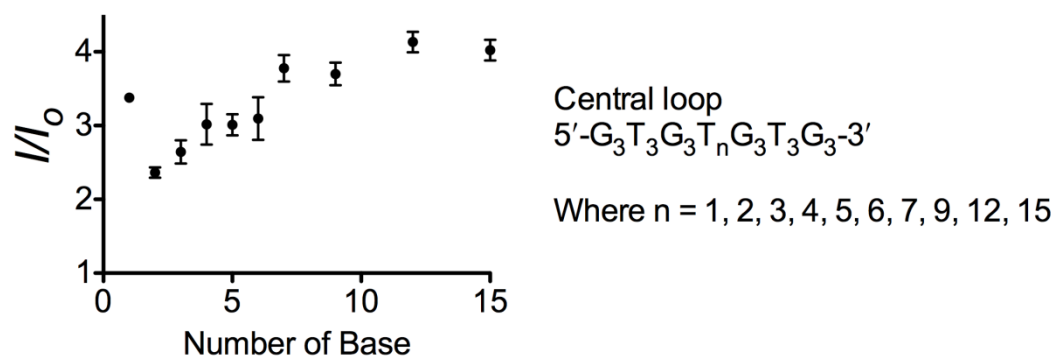


Figure S3 Fold enhancement of complex **1** with or without Pu22 DNA in the presence of increasing concentrations of K^+ .

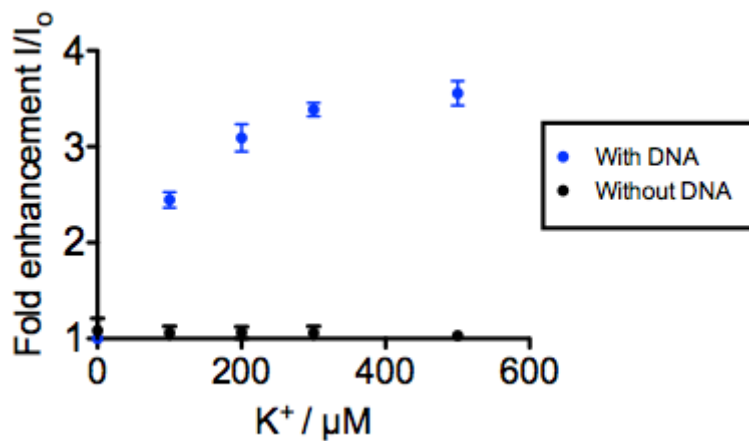


Figure S4 Fold enhancement of complex **1** with or without TdT in the presence of increasing concentrations of K^+ .

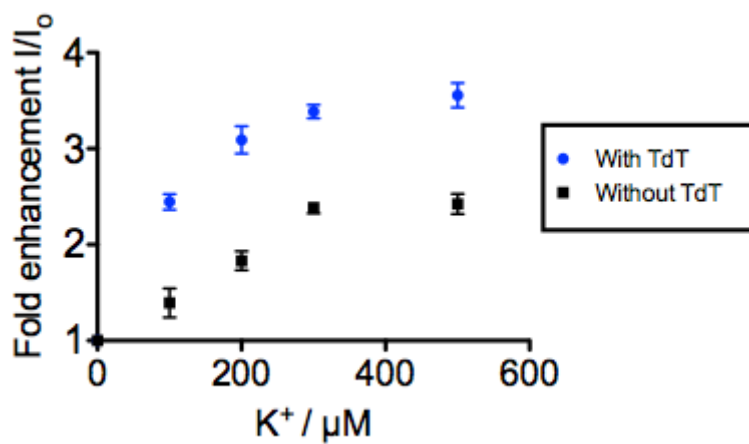


Figure S5 Fold enhancement of the 1/Pu22 (wild-type/mutant) system in response to increasing concentrations of K^+ .

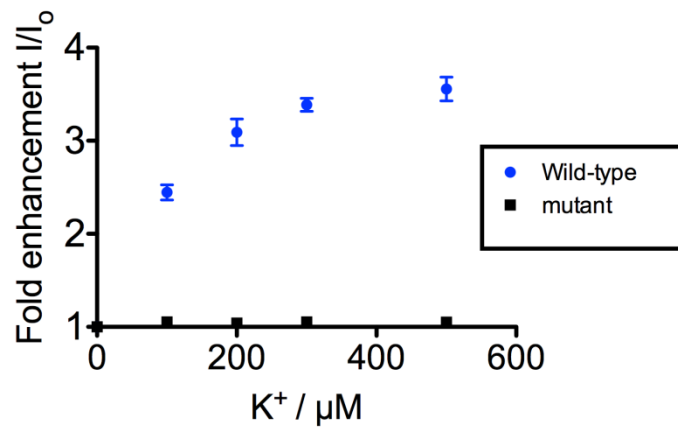


Figure S6 Fold enhancement of the system containing a 100% dTTP pool and 60% dGTP, 40% ATP pool in response to increasing concentrations of K^+ .

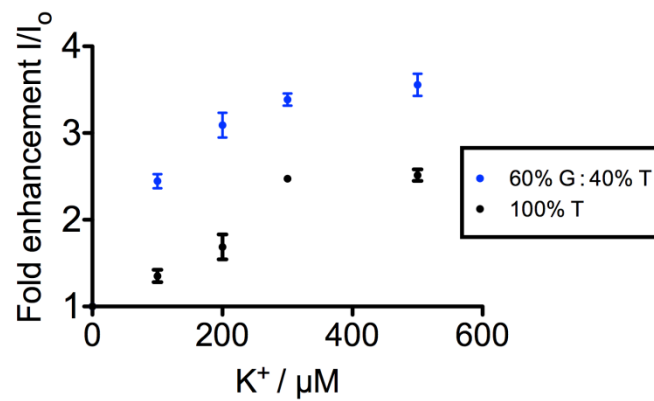


Figure S7 Relative luminescence response of complex **1** towards product DNA produced by increasing concentrations of TdT at 37 °C for 60 min.

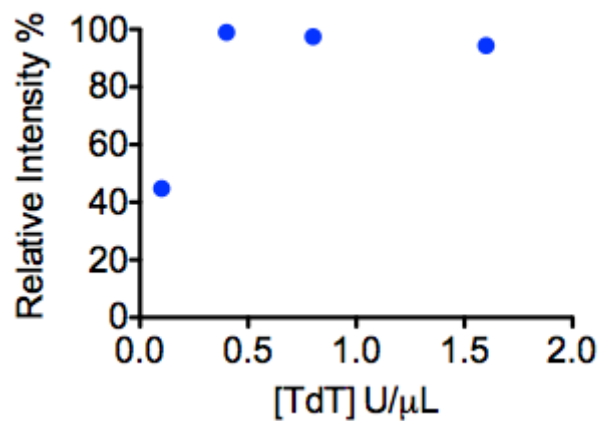


Figure S8 Relative luminescence intensity of the system with different concentrations of KCl (10, 50, 100 and 200 mM).

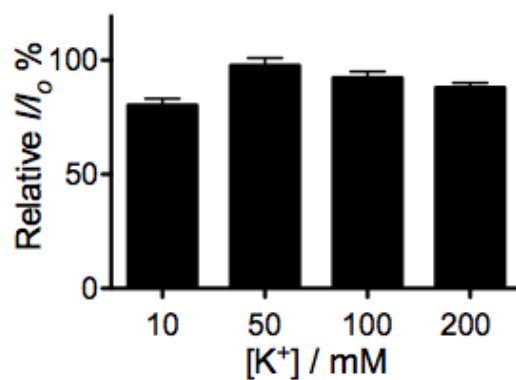


Figure S9 Relative SG intensity in 1 μM K^+ aptamer (Pu22) upon incubation with increasing concentration of ExoI.

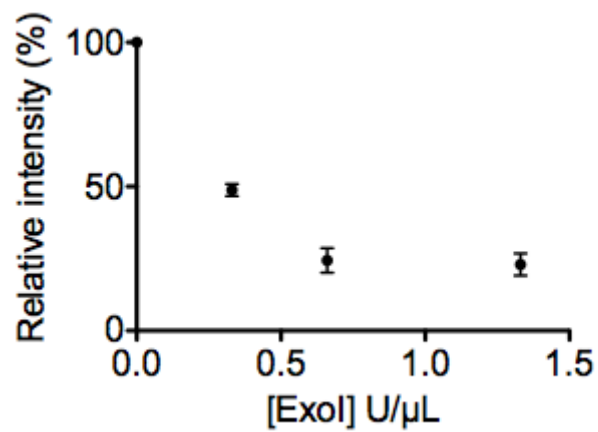


Figure S10 Relative SG intensity in 1 μM thrombin aptamer (TBA) upon incubation with increasing concentration of ExoI.

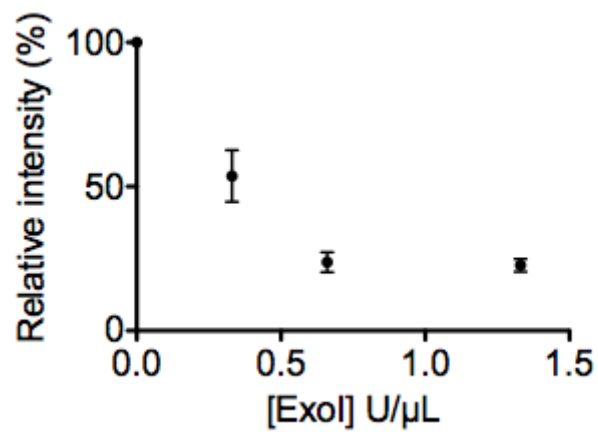


Figure S11 Fold enhancement of complex **1** with or without TdT or DNA in the presence of increasing concentrations of thrombin.

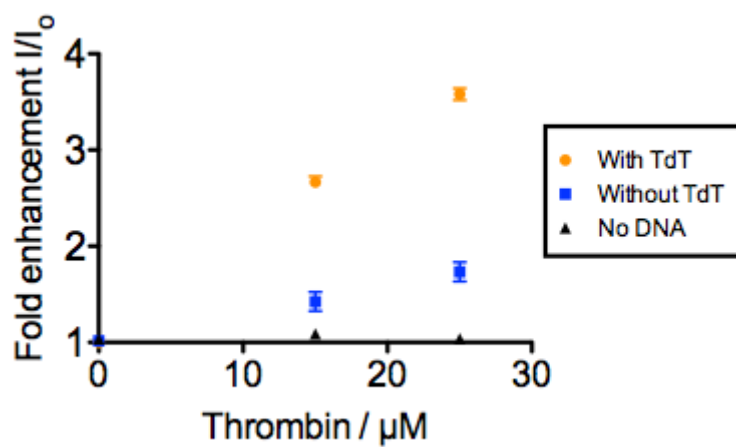


Figure S12 Fold enhancement of the 1/TBA (wild-type/mutant) system in response to increasing concentrations of thrombin.

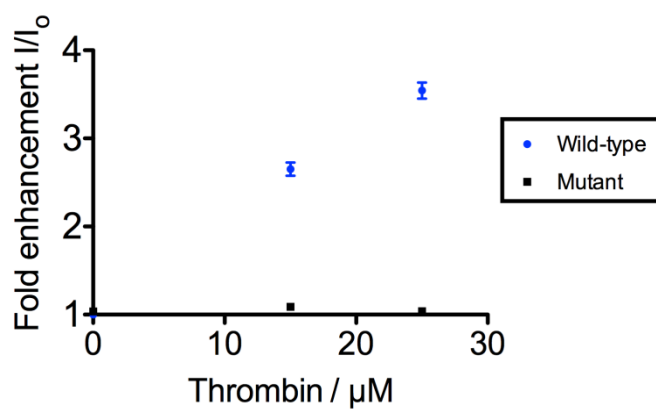


Figure S13 Relative SG intensity in 1 μM cocaine aptamer upon incubation with increasing concentration of ExoI.

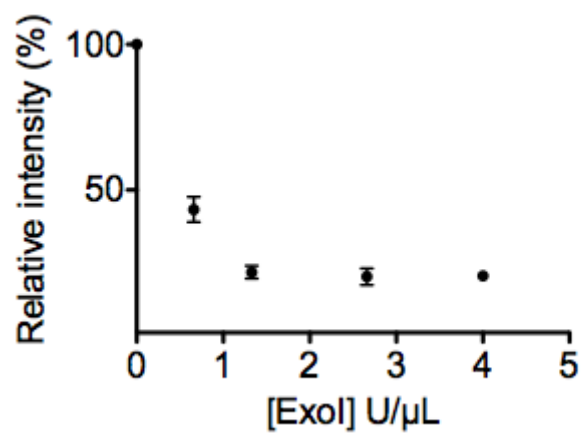


Figure S14 Fold enhancement of complex **1** with or without DNA aptamer in the presence of increasing concentrations of cocaine.

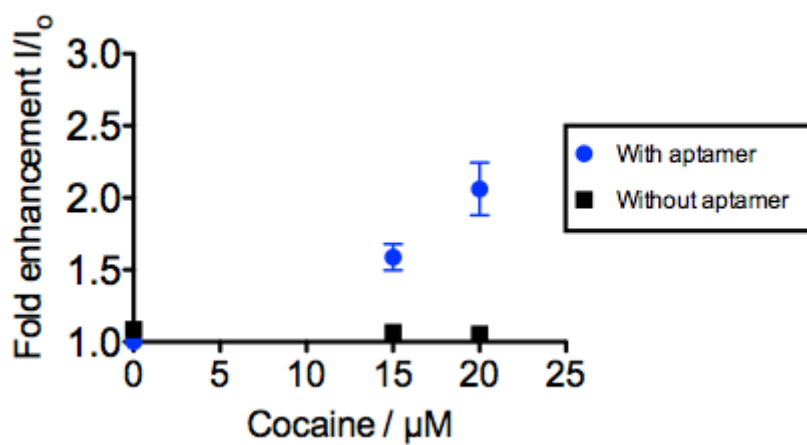


Figure S15 Fold enhancement of the **1**/cocaine aptamer (wild-type/mutant) system in response to increasing concentrations of cocaine.

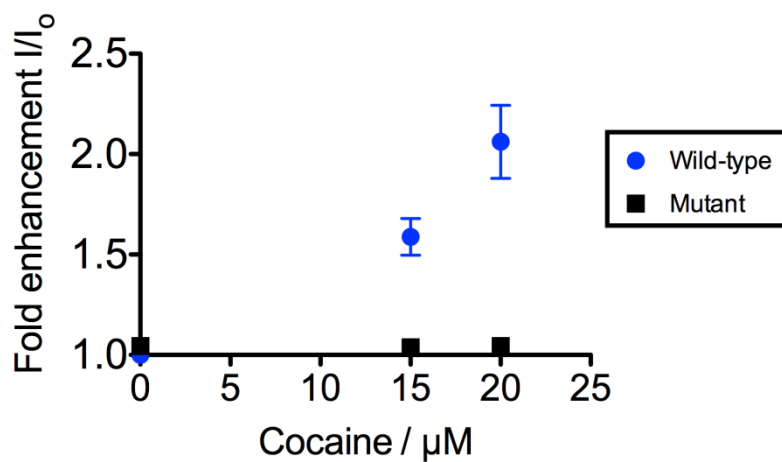


Figure S16 Fold enhancement of the system containing a 100% dTTP pool and 60% dGTP, 40% ATP pool in response to increasing concentrations of cocaine.

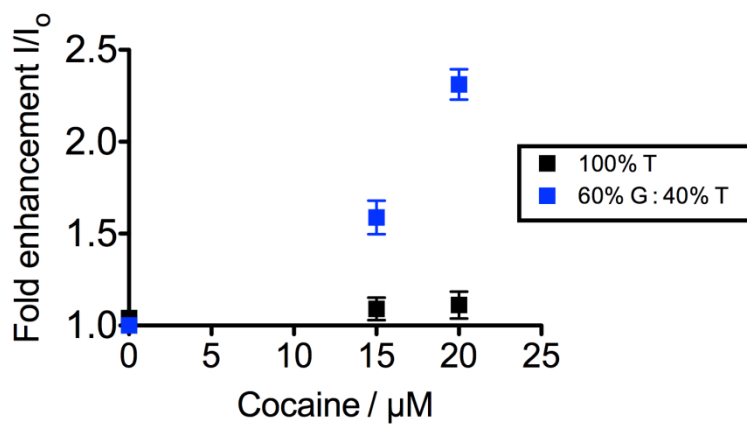


Figure S17 The relationship between luminescence intensity at $\lambda = 637$ nm and cocaine concentration in 50-fold diluted oral fluid sample.

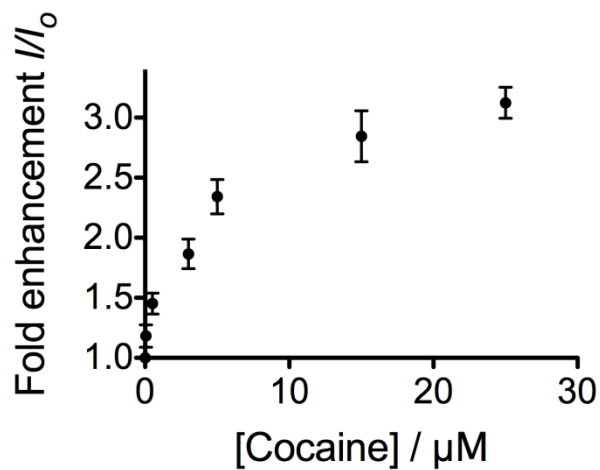


Figure S18 Luminescence intensity of the system in the buffer, cell extract system and buffer system with 20 nM thrombin.

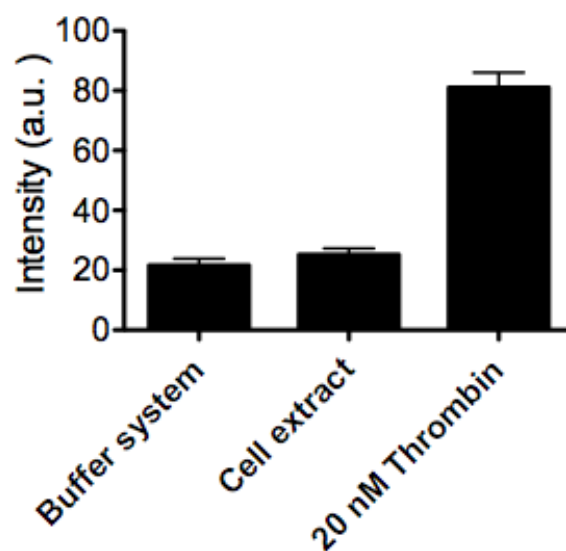
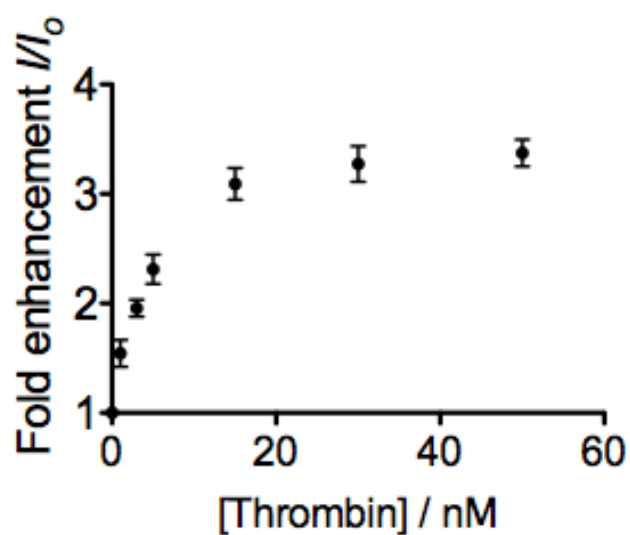


Figure S19 The relationship between luminescence intensity at $\lambda = 637$ nm and thrombin concentration in 0.5% (v/v) cell extract.



References

- (1) Crosby, G. A.; Demas, J. N. Measurement of Photoluminescence Quantum Yields. Review. *J. Phys. Chem.* **1971**, *75*, 991-1024.
- (2) Marmion, C. J.; Griffith, D. M.; Parker, J.; Ude, Z.; Nimir, H.; Morgan, M.; Brennan, M.; Duff, B.; Egan, D.; Chubb, A.; Kasparikova, J.; Brabec, V. Combating Cancer with Precious Metals - A Multi-Functional Approach Towards Developing Novel Anti-Cancer Agents. *J. Biol. Inorg. Chem.* **2014**, *19*, S463-S463.
- (3) Ma, D.-L.; Liu, L.-J.; Leung, K.-H.; Chen, Y.-T.; Zhong, H.-J.; Chan, D. S.-H.; Wang, H.-M. D.; Leung, C.-H. Antagonizing STAT3 Dimerization with a Rhodium(III) Complex. *Angew. Chem. Int. Ed.* **2014**, *53*, 9178-9182.
- (4) Tao, Y.; Lin, Y.; Ren, J.; Qu, X. Self-Assembled, Functionalized Graphene and DNA as a Universal Platform for Colorimetric Assays. *Biomaterials* **2013**, *34*, 4810-4817.
- (5) Zhao, X.-H.; Gong, L.; Zhang, X.-B.; Yang, B.; Fu, T.; Hu, R.; Tan, W.; Yu, R. Versatile DNzyme-Based Amplified Biosensing Platforms for Nucleic Acid, Protein, and Enzyme Activity Detection. *Anal. Chem.* **2013**, *85*, 3614-3620.
- (6) Das, J.; Cederquist, K. B.; Zaragoza, A. A.; Lee, P. E.; Sargent, E. H.; Kelley, S. O. An Ultrasensitive Universal Detector Based on Neutralizer Displacement. *Nat. Chem.* **2012**, *4*, 642-648.

- (7) Liu, X.; Freeman, R.; Willner, I. Amplified Fluorescence Aptamer-Based Sensors Using Exonuclease III for the Regeneration of the Analyte. *Chem. Eur. J.* **2012**, *18*, 2207-2211.
- (8) Li, J.; Fu, H.-E.; Wu, L.-J.; Zheng, A.-X.; Chen, G.-N.; Yang, H.-H. General Colorimetric Detection of Proteins and Small Molecules Based on Cyclic Enzymatic Signal Amplification and Hairpin Aptamer Probe. *Anal. Chem.* **2012**, *84*, 5309-5315.
- (9) Zheng, D.; Zou, R.; Lou, X. Label-Free Fluorescent Detection of Ions, Proteins, and Small Molecules Using Structure-Switching Aptamers, SYBR Gold, and Exonuclease I. *Anal. Chem.* **2012**, *84*, 3554-3560.
- (10) Xia, F.; Zuo, X.; Yang, R.; Xiao, Y.; Kang, D.; Vallée-Bélisle, A.; Gong, X.; Yuen, J. D.; Hsu, B. B. Y.; Heeger, A. J.; Plaxco, K. W. Colorimetric Detection of DNA, Small Molecules, Proteins, and Ions Using Unmodified Gold Nanoparticles and Conjugated Polyelectrolytes. *Proc. Natl. Acad. Sci. U.S.A.* **2010**, *107*, 10837-10841.